

Production and decay of the neutral top-pion in high energy e^+e^- colliders

Chongxing Yue^(a,b), Qingjun Xu^b, Guoli Liu^b, Jiantao Li^b

a: CCAST (World Laboratory) P.O. BOX 8730. B.J. 100080 P.R. China

b:College of Physics and Information Engineering,

Henan Normal University, Xinxiang 453002. P.R.China ^{*†}

November 5, 2018

Abstract

We study the production and decay of the neutral top-pion π_t^0 predicted by topcolor-assisted technicolor(TC2) theory. Our results show that, except the dominant decay modes $b\bar{b}$, $\bar{t}c$ and gg , the π_t^0 can also decay into $\gamma\gamma$ and $Z\gamma$ modes. It can be significantly produced at high energy e^+e^- collider(LC) experiments via the processes $e^+e^- \rightarrow \pi_t^0\gamma$ and $e^+e^- \rightarrow Z\pi_t^0$. We further calculate the production cross sections of the processes $e^+e^- \rightarrow \gamma\pi_t^0 \rightarrow \gamma\bar{t}c$ and $e^+e^- \rightarrow Z\pi_t^0 \rightarrow Z\bar{t}c$. We find that the signatures of the neutral top-pion π_t^0 can be detected via these processes.

PACS number(s): 12.60Nz, 14.80.Mz

^{*}This work is supported by the National Natural Science Foundation of China, the Excellent Youth Foundation of Henan Scientific Committee; and Foundation of Henan Educational Committee.

[†]E-mail:cxyue@pbulic.xxptt.ha.cn

1 Introduction

The cause of electroweak symmetry breaking (EWSB) and the origin of fermion masses are important problems of current particle physics. The standard model (SM) accommodates fermion and weak gauge boson masses by including a fundamental weak doublet of scalar Higgs bosons. However, the SM can not explain dynamics responsible for the generation of mass. Furthermore, the scalar sector suffers from the problems of triviality and unnaturalness. Thus, the SM can only be an effective field theory valid below some high energy scale. Topcolor assisted technicolor (TC2) theory [1] is an attractive scheme in which there is an explicit dynamical mechanism for breaking electroweak symmetry and generating the fermion masses including the heavy top quark mass. In TC2 theory, there are no elementary scalar fields and unnatural or excessive fine-tuning of parameters. Thus, TC2 theory is one of the important promising candidates for the mechanism of EWSB.

In TC2 theory[1], almost all of the top quark mass arises from the topcolor interactions. To maintain electroweak symmetry between top and bottom quarks and yet not generate $m_b \approx m_t$, the topcolor gauge group is usually taken to be a strongly coupled $SU(3) \otimes U(1)$. The $U(1)$ provides the difference that causes only top quark to condense. In order that topcolor interactions be natural, i.e. without introducing large isospin violation, it is necessary that EWSB is still mainly generated by technicolor(TC) interactions. In TC2 theory, extended technicolor(ETC) interactions are still needed to generate the masses of light quarks and contribute a few GeV to m_t , i.e. εm_t [2]. This means that the associated top-pions π_t^0, π_t^\pm are not the longitudinal bosons W and Z , but are separately physically observable objects. Thus, TC2 theory predicts a number of Pseudo Goldstone bosons(PGBs) including the technipions in the TC sector and the top-pions in the topcolor sector. These new particles are most directly related to the dynamical symmetry breaking mechanism. Thus, studying the production and decay of these new particles at high energy colliders will be of special interest.

The production and decay of the technipions have been extensively studied in Ref.[3,4].

The virtual effects of the PGB's(technipions and top-pions) on the processes such as $qq \rightarrow t\bar{t}$, $gg \rightarrow t\bar{t}$, $\gamma\gamma \rightarrow t\bar{t}$, $t \rightarrow cV$, and $e^+\gamma \rightarrow tb\bar{\nu}_e$ have been discussed in the literatures, where the signatures and observability of these new particles were investigated in hadronic colliders[5], $\gamma\gamma$ colliders[6] and $e\gamma$ colliders[7] . In this paper, we will study the production and decay of the neutral top-pion at high energy e^+e^- colliders(LC) and discuss the signatures and observability of the neutral top-pion.

The neutral top-pion π_t^0 , as an isospin-triplet, can couple to a pair of gauge bosons through the top quark triangle loop in an isospin violating way similar to the couplings of QCD pion π^0 to a pair of gauge bosons. Our results indicate that the main contributions to the production cross section of the neutral top-pion π_t^0 are expected to come from the $e^+e^- \rightarrow \pi_t^0\gamma$ channel at the LC experiments. In this channel, we find that several hundred events of π_t^0 can be produced per year by assuming an intergrated luminosity $L = 100fb^{-1}$. Possibly, a smaller π_t^0 production may also be observed in the $e^+e^- \rightarrow \pi_t^0Z$ channel.

For TC2 theory, the underlying interactions, topcolor interactions, are nonuniversal and therefore do not possess a GIM mechanism. This is an essential feature of this kind of models due to the need to single out the top quark for condensation. This nonuniversal gauge interactions result in flavor changing neutral current(FCNC) vertices when one writes the interactions in the quark mass eigen-basis. Thus, the top-pions have large Yukawa coupling to the third family fermions and induce the new flavor changing scalar couplings including the $t - c$ transitions for the neutral top-pion π_t^0 . Within the SM, the flavor changing processes are controlled by the scalar sector and the one-loop level FCNCs are very small. Thus, we can detect the neutral top-pion via the processes $e^+e^- \rightarrow \pi_t^0\gamma \rightarrow \bar{t}c\gamma$ or $e^+e^- \rightarrow \pi_t^0Z \rightarrow \bar{t}cZ$. Our results show that the production cross sections are significantly large and may be observable in the future LC experiments.

In the rest of this paper, we will give our results in detail. The couplings of the neutral top-pion π_t^0 to the ordinary particles are discussed in Sec.2, and the decay widths of the relative decay modes are also estimated. In Sec.3 , we calculate the production cross sections of the processes $e^+e^- \rightarrow \pi_t^0\gamma \rightarrow \bar{t}c\gamma$ and $e^+e^- \rightarrow \pi_t^0Z \rightarrow \bar{t}cZ$. Our conclusions

are given in Sec.4.

2 The couplings of the neutral top-pion π_t^0 to the ordinary particles

To solve the phenomenological difficulties of TC theory, TC2 theory[1] was proposed by combining TC interactions with the topcolor interactions for the third generation at the energy scale of about 1 TeV. In TC2 theory, the TC interactions play a main role in breaking the electroweak gauge symmetry. The ETC interactions give rise to the masses of the ordinary fermions including a very small portion of the top quark mass, namely ϵm_t with a model dependent parameter $\epsilon \ll 1$. The topcolor interactions also make small contributions to the EWSB, and give rise to the main part of the top quark mass, $(1 - \epsilon)m_t$, similar to the constituent masses of the light quarks in QCD. So, for TC2 theory, there is the following relation:

$$\nu_\pi^2 + F_t^2 = \nu_w^2, \quad (1)$$

where ν_π represents the contributions of the TC interactions to the EWSB, $F_t = 50\text{GeV}$ is the top-pion decay constant, and $\nu_w = \nu/\sqrt{2} = 174\text{GeV}$.

For TC2 theory, it generally predicts three top-pions with large Yukawa couplings to the third generation. This induces the new flavor changing scalar couplings. The couplings of the neutral top-pion π_t^0 to the ordinary fermions can be written as[1, 8]:

$$\frac{m_t}{\sqrt{2}F_t} \frac{\sqrt{\nu_w^2 - F_t^2}}{\nu_w} [K_{UR}^{tt} K_{UL}^{tt*} \bar{t}_L t_R \pi_t^0 + K_{UR}^{tc} K_{UL}^{tt*} \bar{t}_L c_R \pi_t^0 + h.c.], \quad (2)$$

where the factor $\frac{\sqrt{\nu_w^2 - F_t^2}}{\nu_w}$ reflects the effect of the mixing between π_t^0 and the would be Goldstone boson [9]. K_{UL}^{ij} is the matrix element of the unitary matrix K_{UL} which the CKM matrix can be derived as $V = K_{UL}^{-1} K_{DL}$ and K_{UR}^{ij} is the matrix element of the right-handed relation matrix K_{UR} . Ref.[8] has shown that their values can be taken as:

$$K_{UL}^{tt} = 1, \quad K_{UR}^{tt} = 1 - \epsilon, \quad K_{UR}^{tc} \leq \sqrt{2\epsilon - \epsilon^2}. \quad (3)$$

If we assume that the part of the top quark mass generated by the topcolor interactions makes up 99% of m_t , i.e. $\epsilon = 0.01$, then we have $K_{UR}^{tc} < 0.14$. In the following calculation, we will take $\epsilon = 0.01$ and K_{UR}^{tc} as a free parameter. The coupling of π_t^0 to the bottom quark can be approximately written as:

$$\frac{m_b - m'_b}{\sqrt{2}F_t} \frac{\sqrt{\nu_w^2 - F_t^2}}{\nu_w} \bar{b}\gamma^5 b \pi_t^0, \quad (4)$$

where m'_b is the ETC generated part of the bottom-quark mass. According to the idea of TC2 theory, the masses of the first and second generation fermions are also generated by ETC interactions. We have $\epsilon m_t = \frac{m_c}{m_s} m'_b$ [10]. If we take $m_s = 0.156 GeV$, $m_c = 1.56 GeV$, then we have $m'_b = 0.1 \times \epsilon m_t$.

The couplings of π_t^0 to gauge bosons via the top quark triangle loop are isospin violating similar to the couplings of QCD pion π^0 to gauge bosons. The general form of the effective $\pi_t^0 - B_1 - B_2$ coupling can be written as [5]:

$$\frac{1}{1 + \delta_{B_1 B_2}} \frac{\alpha S_{\pi_t^0 B_1 B_2}}{\pi F_t} \pi_t^0 \epsilon_{\mu\nu\alpha\beta} (\partial^\mu B_1^\nu) (\partial^\alpha B_2^\beta), \quad (5)$$

where B_1^ν and B_2^β represent the field operators of the gauge bosons. We define α to be the strong coupling constant α_s if B_1 and B_2 are QCD gluons and equal to $\frac{e^2}{4\pi}$ if B_1 and B_2 are electroweak gauge bosons. The anomalous factors $S_{\pi_t^0 B_1 B_2}$ are model dependent. They can be calculated by using the formulas in Ref.[11]. For the neutral top-pion π_t^0 , we have:

$$S_{\pi_t^0 g_a g_b} = \frac{1}{\sqrt{2}} \frac{\sqrt{\nu_w^2 - F_t^2}}{\nu_w} K_{UR}^{tt} J_R, \quad (6)$$

$$S_{\pi_t^0 \gamma \gamma} = \frac{16}{3\sqrt{2}} \frac{\sqrt{\nu_w^2 - F_t^2}}{\nu_w} K_{UR}^{tt} J_R, \quad (7)$$

$$S_{\pi_t^0 Z \gamma} = \frac{16}{3\sqrt{2}} \frac{\sqrt{\nu_w^2 - F_t^2}}{\nu_w} K_{UR}^{tt} \tan \theta_w L(m_{\pi_t}), \quad (8)$$

with

$$L(m_{\pi_t}) = \int_0^1 dx \int_0^1 dy \left[1 + \left(\frac{m_{\pi_t}}{m_t}\right)^2 x(x-1)y^2 + \left(\frac{m_Z}{m_t}\right)^2 yx(y-1) \right]^{-1}, \quad (9)$$

$$J(R_{\pi_t^0}) = \frac{1}{R_{\pi_t^0}^2} \int_0^1 \frac{dx}{x(x-1)} \ln \left[1 - R_{\pi_t^0}^2 x(1-x) \right]. \quad (10)$$

Where $R_{\pi_t^0} = \frac{m_{\pi_t}}{m_t}$, θ_w is the Weinberg angle. In the above formulas, we have ignored the coupling of π_t^0 to a pair of gauge bosons Z and taken $S_{\pi_t^0 ZZ} \approx 0$.

If we assume that the mass of π_t^0 is in the range of $200\text{GeV} \leq m_{\pi_t^0} \leq 350\text{GeV}$ [9], the possible decay modes of π_t^0 are $\bar{t}c$, $b\bar{b}$, gg , $\gamma\gamma$ and $Z\gamma$. Then we have:

$$\Gamma_{total}(\pi_t^0) = \Gamma(\pi_t^0 \rightarrow b\bar{b}) + \Gamma(\pi_t^0 \rightarrow \bar{t}c) + \Gamma(\pi_t^0 \rightarrow gg) + \Gamma(\pi_t^0 \rightarrow \gamma\gamma) + \Gamma(\pi_t^0 \rightarrow Z\gamma). \quad (11)$$

Using Eq.(2)—Eq.(9), we can obtain:

$$\Gamma(\pi_t^0 \rightarrow b\bar{b}) = \frac{3}{16\pi} \frac{\nu_w^2 - F_t^2}{\nu_w^2} \frac{(m_b - 0.1\epsilon m_t)^2}{F_t^2} m_{\pi_t} \sqrt{1 - \frac{4m_b^2}{m_{\pi_t^0}^2}}, \quad (12)$$

$$\Gamma(\pi_t^0 \rightarrow \bar{t}c) = \frac{3(1-\epsilon)^2}{16\pi} \frac{\nu_w^2 - F_t^2}{\nu_w^2} \frac{m_t^2 m_{\pi_t}}{F_t^2} (K_{UR}^{tc})^2 \sqrt{1 - \frac{m_t^2}{m_{\pi_t^0}^2}}, \quad (13)$$

$$\Gamma(\pi_t^0 \rightarrow gg) = \frac{\alpha_s^2(1-\epsilon)^2}{64\pi^3} \frac{m_{\pi_t}^3}{F_t^2} \frac{\nu_w^2 - F_t^2}{\nu_w^2} J^2(R_{\pi_t}), \quad (14)$$

$$\Gamma(\pi_t^0 \rightarrow \gamma\gamma) = \frac{\alpha_e^2(1-\epsilon)^2}{18\pi^3} \frac{\nu_w^2 - F_t^2}{\nu_w^2} \frac{m_{\pi_t}^3}{F_t^2} J^2(R_{\pi_t}), \quad (15)$$

$$\Gamma(\pi_t^0 \rightarrow Z\gamma) = \frac{\alpha_e^2(1-\epsilon)^2}{9\pi^3} \frac{\nu_w^2 - F_t^2}{\nu_w^2} \frac{m_{\pi_t}^3}{F_t^2} \tan^2 \theta_w \left(1 - \frac{m_t^2}{m_{\pi_t^0}^2}\right)^2 L^2(m_{\pi_t}). \quad (16)$$

Since the $\bar{c}_L t_R$ coupling is very small [1, 8], we have assumed $K_{UR}^{tc} \approx K_U^{tc} = \sqrt{|K_{UL}^{tc}|^2 + |K_{UR}^{tc}|^2}$ in Eq.(13). Using above equations, we can estimate the branching ratios of the various decay modes of the neutral top-pion π_t^0 . In Fig.1, we plot the resulting branching ratios as a function of m_{π_t} for $K_{UR}^{tc} = 0.05$. The branching ratios of anomalous channels $\pi_t^0 \rightarrow \gamma\gamma$ and $\pi_t^0 \rightarrow Z\gamma$ are very small, so we do not give the values of $B_r(\gamma\gamma)$ and $B_r(Z\gamma)$ in Fig.1. From Fig.1, we can see that the largest branching ratio is that of the decay channel $\pi_t^0 \rightarrow \bar{t}c$. The $\pi_t^0 \rightarrow \bar{t}c$ branching ratio varies between 46% and 65% for its mass in the range of $200\text{GeV}-350\text{GeV}$. For large value of the π_t^0 mass, a considerable ratio of the π_t^0 decay mode can also occur in the anomalous channel $\pi_t^0 \rightarrow gg$. For $m_{\pi_t} = 300\text{GeV}$, we have $B_r(gg) \simeq 16\%$.

To see the effect of the parameter K_{UR}^{tc} on the branching ratio $B_r(\bar{t}c)$, we plot $B_r(\bar{t}c)$ versus K_{UR}^{tc} in Fig.2 for $m_{\pi_t} = 300\text{GeV}$. From Fig.2 we can see that $B_r(\bar{t}c)$ is sensitive to the value of parameter K_{UR}^{tc} . For $\epsilon > 0.01$, we have $B_r(\bar{t}c) \geq 99\%$.

3 the π_t^0 production at high energy e^+e^- colliders

From above discussion, we can see that gg is one of the dominant decay modes of the neutral top-pion π_t^0 . This will make π_t^0 observed in the $\bar{t}c$ final state at a hadron collider very easy. Ref.[8] has extensively studied the signatures of the π_t^0 at the hadron colliders. In this section we will focus on the π_t^0 production at the high energy e^+e^- colliders(LC). In the LC experiments, the π_t^0 production channels are represented by the processes

$$e^+e^- \rightarrow \pi_t^0\gamma, \quad e^+e^- \rightarrow \pi_t^0Z. \quad (17)$$

For the processes in Eq.(17), the general form of the total cross section has been given in Ref.[12]. For the neutral top-pion π_t^0 , we have assumed that its mass is in the range of $200\text{GeV} \leq m_{\pi_t} \leq 350\text{GeV}$ and $S_{\pi_t^0 ZZ} = 0$. Thus the production cross sections of the processes in Eq.(17) can be written as:

$$\begin{aligned} \sigma(e^+e^- \rightarrow \pi_t^0\gamma) &= \frac{\alpha^3}{24\pi^2 F_t^2} \left(1 - \frac{m_{\pi_t}^2}{S}\right)^3 \\ &\quad \left[S_{\pi_t^0\gamma\gamma}^2 + \frac{(1 - 4S_W^2 + 8S_W^4)}{8S_W^2 C_W^2} \frac{S_{\pi_t^0\gamma Z}^2}{(1 - \frac{m_Z^2}{S})^2} + \frac{1 - 4S_W^2}{2S_W C_W} \frac{S_{\pi_t^0\gamma\gamma} S_{\pi_t^0\gamma Z}}{1 - \frac{m_Z^2}{S}} \right], \\ \sigma(e^+e^- \rightarrow \pi_t^0 Z) &= \frac{\alpha^3}{24\pi^2 F_t^2} \left(1 - \frac{m_{\pi_t}^2}{S} - \frac{m_Z^2}{S}\right)^3 S_{\pi_t^0 Z\gamma}^2, \end{aligned} \quad (18)$$

where \sqrt{S} is the center-of-mass energy. Using the above equations, we can calculate the π_t^0 production cross sections via the processes $e^+e^- \rightarrow \gamma\pi_t^0$ and $e^+e^- \rightarrow Z\pi_t^0$. Our results are shown in Fig.3 as a function of m_{π_t} for $\sqrt{S} = 500\text{GeV}$, $\epsilon = 0.01$. From Fig.3, we can see that the production cross sections increase with decreasing the value of m_{π_t} in most of the parameter space and the cross section $\sigma_{\gamma\pi_t^0}$ is larger than the cross section $\sigma_{Z\pi_t^0}$. However, the cross section $\sigma_{\gamma\pi_t^0}$ increases with increasing the mass m_{π_t} for $m_{\pi_t} > 320\text{GeV}$. The reason is that the factor $S_{\pi_t^0\gamma\gamma}$ increases speedily as $R_{\pi_t^0} = \frac{m_{\pi_t}}{m_t}$ goes to $R_{\pi_t^0} = 2$. For $m_{\pi_t} = 300\text{GeV}$, the cross sections are $\sigma_{\gamma\pi_t^0} = 2.5\text{fb}$ and $\sigma_{Z\pi_t^0} = 0.47\text{fb}$. To see the effects of the center-of-mass energy \sqrt{S} on the production cross sections, we plot the cross section $\sigma_{\pi_t^0\gamma(Z)}$ versus \sqrt{S} in Fig.4 for $\epsilon = 0.01$ and $m_{\pi_t} = 300\text{GeV}$. From Fig.4, we can see that the cross sections increase with increasing the value of \sqrt{S} . For the process $e^+e^- \rightarrow \pi_t^0\gamma$, the cross section increases from 2.5fb to 7.1fb as \sqrt{S} increases from 500GeV to 1000GeV .

We consider two future e^+e^- collider scenarios: a LC with $\sqrt{S} = 500\text{GeV}$ and a yearly integrated luminosity of $L = 50\text{fb}^{-1}$ and a LC with $\sqrt{S} = 1000\text{GeV}$ and $L = 100\text{fb}^{-1}$. The yearly production events can be easily calculated. Our numerical results are shown in Table 1. From Table 1 we can see that the neutral top-pion π_t^0 can be significantly produced via the $e^+e^- \rightarrow \pi_t^0\gamma$ channel at the future high energy e^+e^- colliders. For this channel, several hundred events of π_t^0 can be produced per year which would be observed at the LC experiments, π_t^0 can also be produced via the $e^+e^- \rightarrow \pi_t^0 Z$ channel. Several ten events of π_t^0 can be produced per year which may be observed at the LC experiments with $\sqrt{S} = 1000\text{GeV}$.

Table 1: The number of π_t^0 produced per year from $\pi_t^0\gamma$ and $\pi_t^0 Z$ at the LC experiments

\sqrt{s}	$m_{\pi_t} = 250\text{GeV}$	$m_{\pi_t} = 300\text{GeV}$	$m_{\pi_t} = 350\text{GeV}$
	$\{\pi_t^0\gamma, \pi_t^0 Z\}$	$\{\pi_t^0\gamma, \pi_t^0 Z\}$	$\{\pi_t^0\gamma, \pi_t^0 Z\}$
500GeV	150, 31	125, 23	163, 22
1000GeV	582, 136	713, 153	1650, 269

In the SM, $\bar{t}c$ pair production cross sections are unobservably small due to the unitarity of CKM matrix [13]. Thus, any signal of such $t - c$ transitions will be a clear evidence of new physics beyond the SM. This fact has led to a lot of theoretical activities involving $t - c$ transitions within some specific popular models beyond the SM. For example, $\bar{t}c$ production has been studied in Multi Higgs doublets models [14], in supersymmetry with R-Parity violation [15], in models with extra vector-like quarks [16] and model independent[17]. For TC2 models, we have discussed the contributions of the new gauge bosons and the neutral top-pion π_t^0 to $\bar{t}c$ production[18]. From our discussion in Sec.2, we can see that the $\bar{t}c$ mode is one of the dominant decay modes of the neutral top-pion π_t^0 . Thus the new flavor changing scalar coupling $\pi_t^0\bar{t}c$ may have significant contributions to the processes $e^+e^- \rightarrow \gamma\pi_t^0 \rightarrow \gamma\bar{t}c$ and $e^+e^- \rightarrow Z\pi_t^0 \rightarrow Z\bar{t}c$. The neutral top-pion π_t^0 may be detected by studying these processes. Since we only consider the real π_t^0 production,

the cross sections of the processes $e^+e^- \rightarrow \gamma\bar{t}c$ and $e^+e^- \rightarrow Z\bar{t}c$ contributed by π_t^0 can be written as:

$$\sigma_{\gamma\bar{t}c} \approx \sigma(e^+e^- \rightarrow \gamma\pi_t^0) \times B_r(\bar{t}c), \quad (20)$$

$$\sigma_{Z\bar{t}c} \approx \sigma(e^+e^- \rightarrow Z\pi_t^0) \times B_r(\bar{t}c), \quad (21)$$

with

$$B_r(\pi_t^0 \rightarrow \bar{t}c) = \frac{\Gamma(\pi_t^0 \rightarrow \bar{t}c)}{\Gamma_{total}(\pi_t^0)}. \quad (22)$$

Where $\Gamma_{total}(\pi_t^0)$ is the total decay width of the π_t^0 . In Fig.5, we plot the cross sections $\sigma_{\gamma\bar{t}c}$ and $\sigma_{Z\bar{t}c}$ as a function of the mass m_{π_t} for $\sqrt{S} = 500\text{GeV}$, in which the solid and dotted lines stand for the final states $\gamma\bar{t}c$ and $Z\bar{t}c$, respectively. From Fig.5 we can see that, for $200\text{GeV} \leq m_{\pi_t} \leq 350\text{GeV}$, the cross section $\sigma_{\gamma\bar{t}c}$ varies from 1.29fb to 2.05fb and $\sigma_{Z\bar{t}c}$ varies from 0.20fb to 0.45fb . Thus, for a LC with $\sqrt{S} = 500\text{GeV}$, TC2 models predict tens and up to one hundred of $\gamma\bar{t}c$ raw events, and only few of $Z\bar{t}c$ raw events. Detecting the neutral top-pion π_t^0 is very difficult via the process $e^+e^- \rightarrow Z\pi_t^0 \rightarrow Z\bar{t}c$. However, we can study the signature and observability of π_t^0 via the process $e^+e^- \rightarrow \gamma\pi_t^0 \rightarrow \gamma\bar{t}c$ and further test TC2 models. In Fig.6 we show the $\sigma_{\gamma\bar{t}c}$ and $\sigma_{Z\bar{t}c}$ as a function of \sqrt{S} for $m_{\pi_t} = 300\text{GeV}$. Same as Fig.5, the solid and dotted lines stand for the final states $\gamma\bar{t}c$ and $Z\bar{t}c$, respectively. From Fig.6, we can see that the cross sections increase with increasing \sqrt{S} . For a LC with $\sqrt{S} = 1000\text{GeV}$ and $L = 100\text{fb}^{-1}$, there can be about 443 $\gamma\bar{t}c$ raw events and 95 $Z\bar{t}c$ raw events for $m_{\pi_t} = 300\text{GeV}$. Thus, the neutral top-pion π_t^0 can also be detected via the process $e^+e^- \rightarrow Z\bar{t}c$ at a LC with $\sqrt{S} = 1000\text{GeV}$.

4 summary

To avoid or solve the problems, such as triviality and unnaturalness arising from the elementary Higgs field, various kinds of dynamical electroweak symmetry breaking models have been proposed, and among which TC2 theory is one of the important candidates. TC2 theory predicts the existence of the top-pions. These new particles are most directly related to the dynamical symmetry breaking mechanism and can be seen as the charac-

teristic feature of TC2 theory. Thus it is of great importance to understand what about the prospects for discovering the top-pions and whether we can study their properties to determine key features and parameters of TC2 theory.

In this paper, we have studied the production and decay of the neutral top-pion π_t^0 at high-energy e^+e^- colliders. The top-pions have large Yukawa couplings to the third generation fermions and induce the new flavor changing scalar couplings including the $\pi_t^0 \bar{t}c$ coupling for the neutral top-pion π_t^0 . The neutral top-pion π_t^0 , as an isospin-triplet, can couple to a pair of gauge bosons through the top quark triangle loop in an isospin violating way similar to the couplings of QCD pion π^0 to a pair of gauge bosons. Our results indicate that the dominant decay modes are $\bar{t}c$ and gg . Thus, the π_t^0 can be significantly produced at hadronic colliders. The signatures and observability of the neutral top-pion π_t^0 can be studied at the Tevatron. This is consistent with the results of Ref.[8].

Except the decay modes $\bar{t}c$ and gg , the π_t^0 can also decay into $\gamma\gamma$ and $Z\gamma$ modes. Thus, the π_t^0 can be produced at the LC experiments via the processes $e^+e^- \rightarrow \pi_t^0\gamma$ and $e^+e^- \rightarrow Z\pi_t^0$. For $\sqrt{S} = 1000\text{GeV}$, the production cross sections $\sigma_{\pi_t^0\gamma}$ and $\sigma_{\pi_t^0 Z}$ can reach 7.1fb and 1.5fb , respectively. It is expected that there will be several hundreds $\gamma\pi_t^0$ and $Z\pi_t^0$ events per year at the LC experiments with $\sqrt{S} = 1000\text{GeV}$. Thus the neutral top-pion π_t^0 will be observed at the high energy e^+e^- colliders.

Since the $\bar{t}c$ production cross sections are unobservably small in the SM, any signal of $\bar{t}c$ production will be a clear evidence of new physics beyond the SM. The flavor changing scalar coupling $\pi_t^0 \bar{t}c$ has significant contributions to the processes $e^+e^- \rightarrow \gamma\pi_t^0 \rightarrow \gamma\bar{t}c$ and $e^+e^- \rightarrow Z\pi_t^0 \rightarrow Z\bar{t}c$. The neutral top-pion π_t^0 can be detected by studying these processes. Furthermore, we can test TC2 models via these processes at the high-energy e^+e^- colliders.

Figure captions

Fig.1: The branching ratios of the neutral top-pion as a function of its mass m_{π_t} .

Fig.2: The branching ratio $B_r(\pi_t^0 \rightarrow \bar{t}c)$ versus the free parameter K_{UR}^{tc} for the mass $m_{\pi_t} = 300GeV$.

Fig.3: The production cross sections $\sigma_{\gamma\pi_t^0}$ and $\sigma_{Z\pi_t^0}$ of the neutral top-pion π_t^0 as a function of its mass for $\sqrt{S} = 500GeV$.

Fig.4: The production cross sections $\sigma_{\gamma\pi_t^0}$ and $\sigma_{Z\pi_t^0}$ versus the center-of-mass energy \sqrt{S} for $m_{\pi_t} = 300GeV$.

Fig.5: The cross sections $\sigma_{\gamma\bar{t}c}$ and $\sigma_{Z\bar{t}c}$ versus the mass m_{π_t} for $\sqrt{S} = 500GeV$.

Fig.6: The cross sections $\sigma_{\gamma\bar{t}c}$ and $\sigma_{Z\bar{t}c}$ versus \sqrt{S} for $m_{\pi_t} = 300GeV$.

References

- [1] C.T.Hill, *Phys. Lett.* **B345**, 483(1995); K. Lane and E. Eichten, *Phys. Lett.* **B352**, 382(1995); K. Lane, *Phys. Lett.* **B433**, 96(1998).
- [2] G.Buchalla, G. Burdman, C. T. Hill and D. Kominis, *Phys. Rev.* **D53**, 5185(1996).
- [3] V. Lubicz, *Nucl. Phys.* **B404**, 559(1993); V. Lubicz and P. Santorelli, *Nucl. Phys.* **B460**, 3(1996); R. Casalbuoni, A. Deandrea, S. D. Curtis, D. Dominici, R. Gatto, and J. F. Gunion, *Nucl. Phys.* **B555**, 3(1999).
- [4] R. S. Chivukula, R. Rosenfeld, E. H. Simmons and J. Terning, hep-ph/9503202; K. Lane, *Phys. Lett.* **B357**, 624(1995); E. Eichten, K. Lane and J. Womersley, *Phys. Lett.* **B405**, 305(1997).
- [5] E. Eichten and K. Lane, *Phys. Lett.* **B327**, 129(1994); G. L. Lu, H. Yang, J. M. Yang, and X. L. Wang, *Phys. Rev.* **D54**, 1083(1996); Chongxing Yue, Hongyi Zhou, Yuping Kuang, and Gongru Lu, *Phys. Rev.* **D55**, 5541(1997).
- [6] Hongyi Zhou, Yuping Kuang, Chongxing Yue and Hua Wang, *Phys. Rev.* **D57**, 4205(1998).
- [7] Xuelei Wang, et al, *Phys. Rev.* **D60**, 014002(1999).
- [8] Hong-Jian He and C. P Yuan, *Phys. Rev. Lett.* **83**, 28(1999); G. Burdman, *Phys. Rev. Lett.* **83**, 2888(1999).
- [9] G. Burdman and D. Kominis, *Phys. Lett.* **B403**, 101(1997); W. Loinaz and T. Takuchi, *Phys. Rev.* **D60**, 015005(1999); Chongxing Yue, Yuping Kuang, Xuelei Wang, and Weibin Li, *Phys. Rev.* **D62**, 055005(2000).
- [10] Chongxing Yue, Yuping Kuang and Gongru Lu, *J. Phys.* **G23**, 163(1997).
- [11] D. Slaven, Bing-Ling Yang, and X. M. Zhang, *Phys. Rev.* **D45**, 4349(1992); Chongxing Yue, Xuelei Wang, and Gongru Lu, *J. Phys* **G19**, 821(1993).

- [12] L. Randall and E. H. Simmons, *Nucl. Phys. B***380**, 3(1992).
- [13] G. Eilam, *Phys. Rev. D***18**, 1202(1983); C.H. Chang, et al, *Phys. Lett. B***313**, 389(1993); C. S. Huang, X. H. Wu. and S. H. Zhu, *Phys. Lett. B***452**, 143(1999).
- [14] D. Atwood, L. Reina and A. Soni, *Phys. Rev. D***55**, 3156(1997); S. Bar-Shalom, G. Eilam, A. Soni and J. Wudka, *Phys. Rev. Lett.***79**, 1217(1997); *ibid. Phys. Rev. D***57**, 2957(1998); J. Yi et al, *Phys. Rev. D***57**, 4343(1998); W.-S. Hou, G.-L. Lin and C.-Y. Ma, *Phys. Rev. D***56**, 7434(1997); M. Sher, hep-ph/9809590.
- [15] U. Mahanta and H. Ghosal, *Phys. Rev. D***57**, 1735(1998); S. Bar-Shalom, G. Eilam and A. Soni, *Phys. Rev. D***59**, 035010(1999); M. Chemtob and G. Moreau, *Phys. Rev. D***59**, 116012(1999); Z.-H. Yu et al, *Eur. Phys. J. C***16**, 541(2000).
- [16] F. del Aguila, J. A. Aguilar-Saavedra and R. Miquel, *Phys. Rev. Lett.* **82**,1628(1999).
- [17] T. Han and J. L. Hewett, *Phys. Rev. D***60**, 074015(1999); S. Bar-Shalom and J. Wudka, *Phys. Rev. D***60**, 094016(1999).
- [18] Chongxing Yue and Weibin Li, *Mod. Phys. Lett. A***15**, 361(2000); Chongxing Yue, et al, hep-ph/0011112(to be published in *Phys. Lett. B*).

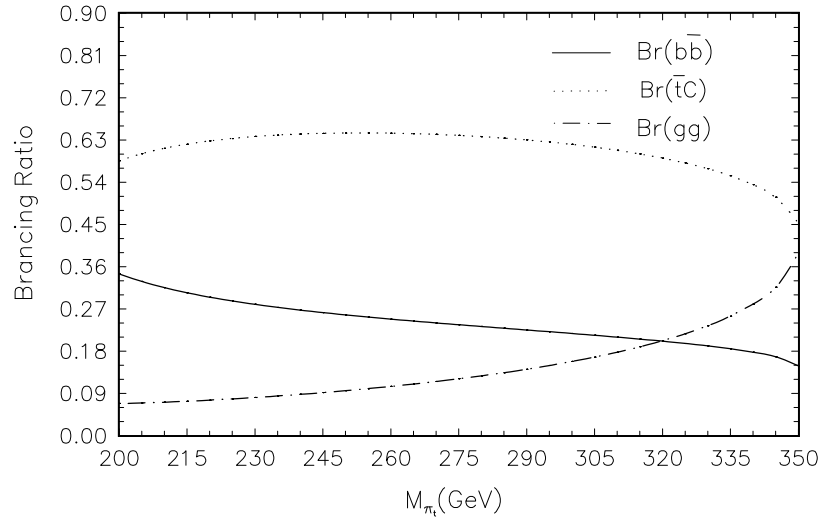


Fig.1

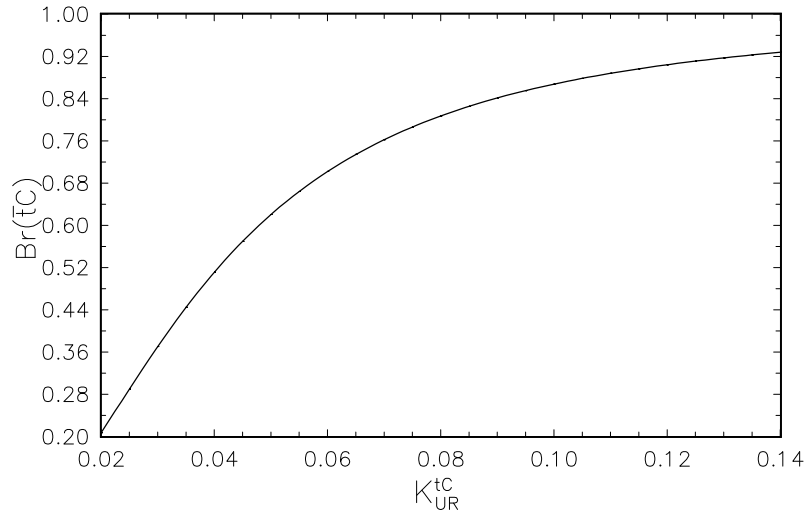


Fig.2

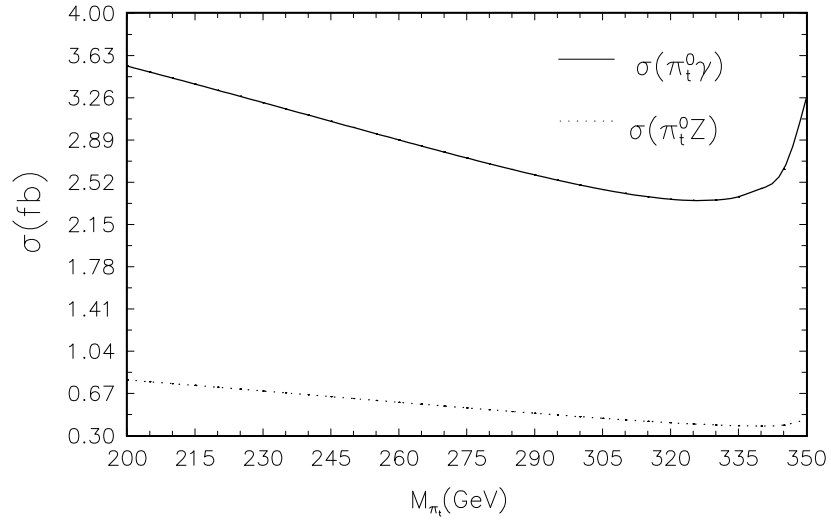


Fig.3

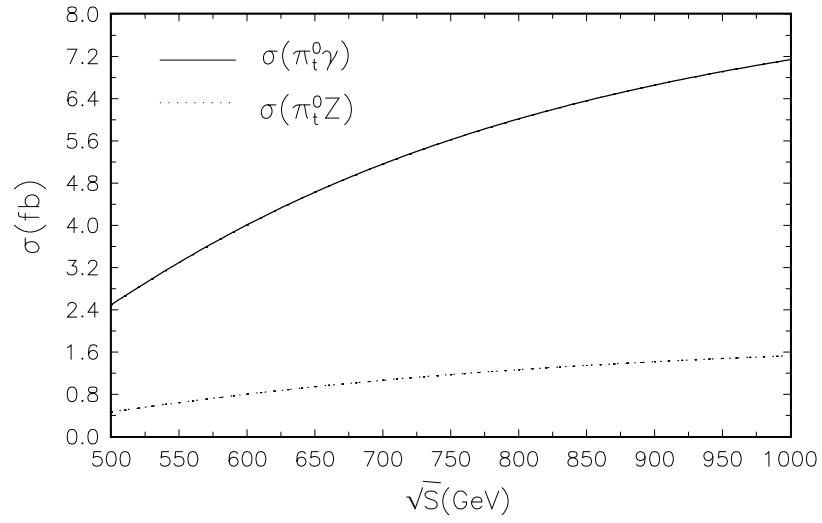


Fig.4

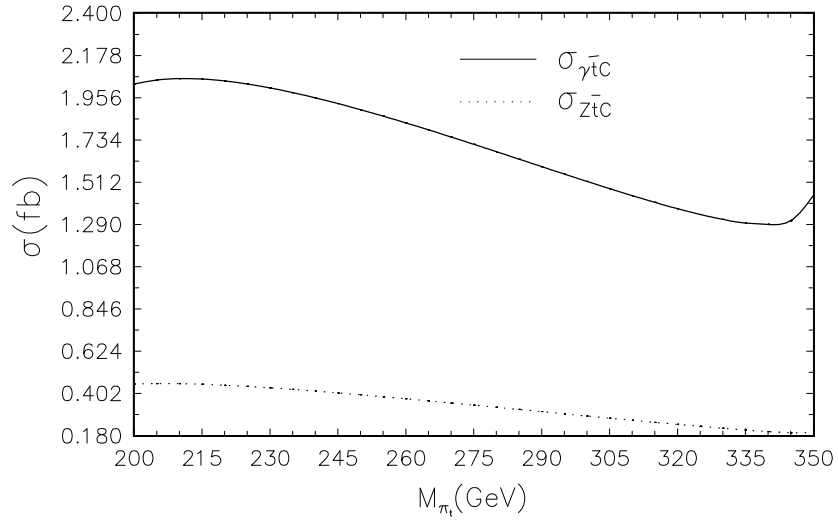


Fig.5

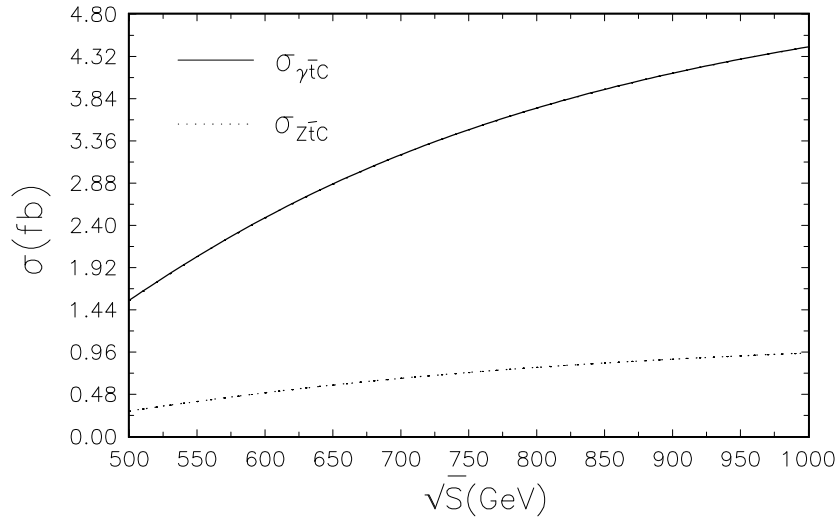


Fig.6